ANNUAL REVIEWS

Annual Review of Earth and Planetary Sciences

Clocks in Magmatic Rocks

Fidel Costa

Asian School of the Environment and Earth Observatory of Singapore, Nanyang Technological University, Singapore 639798; email: fcosta@ntu.edu.sg

Annu. Rev. Earth Planet. Sci. 2021. 49:231–52

First published as a Review in Advance on December 8, 2020

The *Annual Review of Earth and Planetary Sciences* is online at earth.annualreviews.org

https://doi.org/10.1146/annurev-earth-080320-060708

Keywords

volcanology, geochemistry, mineralogy, thermodynamics, kinetics, radioactivity

Abstract

Understanding the evolution and processes that shape our planet critically depends on the robustness of the absolute ages and process durations obtained from rocks and crystals. Two main aspects of time information on magmatic systems are currently at the forefront of new knowledge. The capacity to determine process durations on human timescales makes it possible to relate the magma dynamics below active volcanoes with the monitoring signals measured at the surface, thereby improving eruption hazards mitigation. The combination of precise in situ dating of accessory minerals and diffusion chronometry is unraveling the incremental growth of large silica-rich magma reservoirs over thousands to hundreds of thousands of years and illuminates the complex relationships between plutonic and volcanic systems. Further progress could be made by decreasing the volume of the analyzed crystals and the error of time determinations, addressing the crystal representativeness and sampling bias, and connecting the time information with physicochemical models of magmatic systems.

- Rock-forming minerals are time capsules of magmatic processes that occur on human timescales and can help to better anticipate volcanic eruptions.
- In situ dating of accessory minerals reveals that large magma reservoirs evolve through multiple thermal fluctuations of over tens to hundreds of thousands of years.
- Progress on conceptual models of magma storage and rejuvenation requires improved error analysis of timescales and representativeness of crystal populations.

1. INTRODUCTION

Determining the ages of rocks and crystals is essential to understanding Earth's origin, how it has evolved through time, and how it currently works (e.g., MacDougall 2008). Quantification of the timing and rates of erosion, mountain building, metamorphism and igneous intrusions, the creation of the oceanic crust, and the frequency of large volcanic eruptions provides the basic information to understand the processes that shape our planet (e.g., Reiners et al. 2018). Improved analytical techniques over the past three decades have made it possible to determine the isotopic and elemental concentrations of an increased number of elements, in minerals, glass, and rocks, using incredibly small sample volumes (e.g., Reiners et al. 2018). This has facilitated much better constraints on the ages and durations of a range of processes, including those related to magmatic rocks, which are the main subject of this review (e.g., Dosseto et al. 2010) (**Figure 1**). For example, the improved precision of zircon ages has led to the quantification of the rates of incremental emplacement of plutonic complexes in the continental crust on timescales of less than a few million years (e.g., Schalttegger & Davies 2017). In the volcanic realm, precise time information from crystals has shown that although crystal-rich magma silicic reservoirs are built over hundreds of thousands of years, they can be primed for eruption in a few decades or less (e.g., Cooper 2015) (**Figure 1**). Short times of a few weeks to decades have been obtained for magma replenishment, storage, and degassing of mafic subvolcanic reservoirs (e.g., Costa et al. 2020) (**Figure 1**).

In many of these studies, the time is obtained from single crystals, and a general finding of the past decades is that a single hand specimen of a volcanic or plutonic rock can contain crystal populations of different origins and age ranges (e.g., Bacon & Lowenstern 2005) (**Figure 2**). The

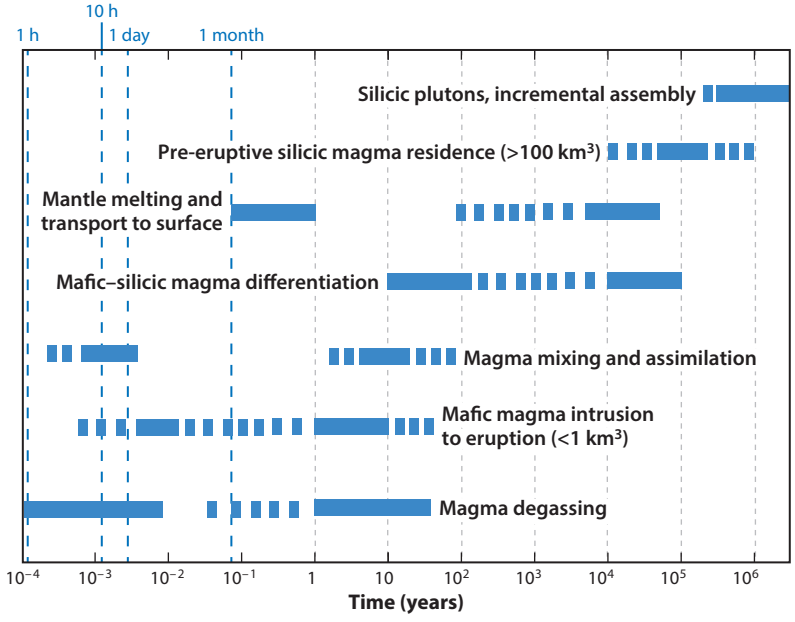

Figure 1

Synthetic and simplified summary of the ranges of timescales that have been determined in the past decades for a variety of magmatic processes. Note the large ranges of timescales, from volcanic degassing to pluton emplacement and large silicic calderas. Although not apparent in this figure, there is also a general relation of increasing timescales from more mafic to more silicic magmas, and from small to large magmatic systems. Figure adapted with permission from Cooper (2015, 2019), Costa et al. (2020), and Turner & Costa (2007).

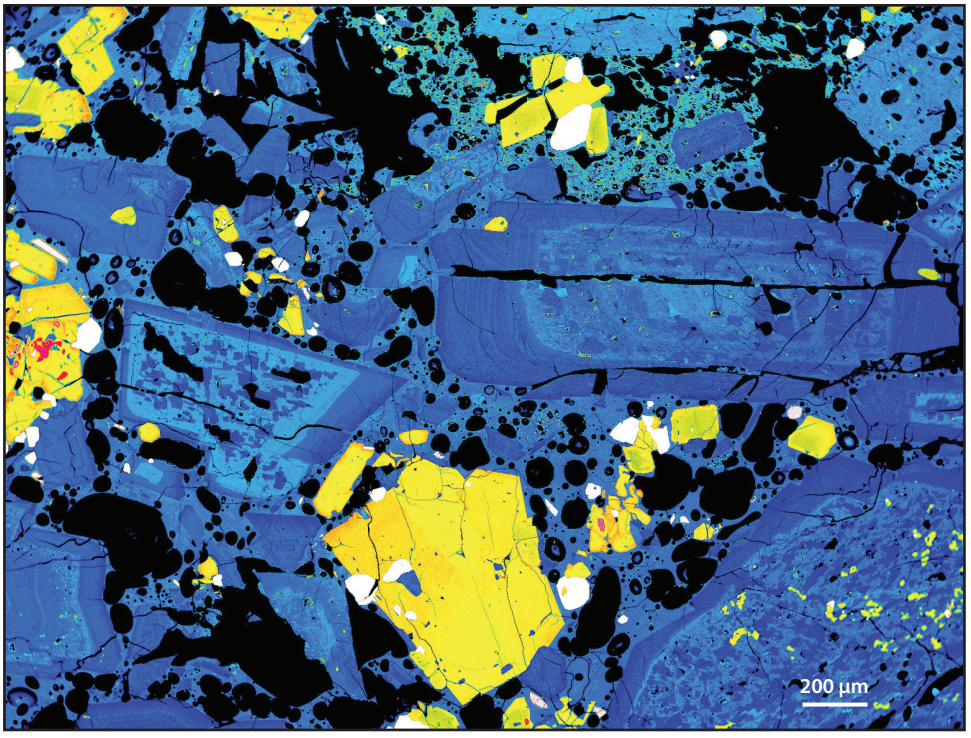

Figure 2

Two-dimensional X-ray map (false color image) of a basaltic andesite sample from Mayon volcano (Luzon arc, Philippines). The rock contains a varied mineral assemblage and a range of crystals with different textures and zoning patterns. The blue colors are mainly plagioclase and matrix glass, with lighter blue areas indicative of higher Ca contents than darker blue areas. The yellow and red colors are pyroxene crystals, and the white are Fe–Ti oxide crystals; empty vesicles and cracks are in black. The challenge is to be able to unravel the ages and timescales recorded in the different crystals. Unfortunately, it is not possible to determine the age of each crystal zone precisely enough to determine when they grew or how many are recycled from previous eruptions. Much time and many financial resources are currently used to unravel the time information from different crystal populations using isotope studies (e.g., Davidson et al. 2007) or using statistical analysis of major elements from hundreds of crystals (Cheng & Costa 2019). Figure courtesy of D. Ruth.

variety of crystal populations may be the result of interactions between magmas originating from the lower crust to the shallow subvolcanic reservoirs (e.g., Cashman et al. 2017), and much effort and many financial resources are currently used to untangle the various crystal populations, ranges of crystal ages, and their origins (e.g., Cheng & Costa 2019, Davidson et al. 2007).

This article reviews some recent findings related to the timescales of magmatic systems. The objective is not to provide an exhaustive manual for the approaches or detailed data sets but to highlight some of the recent ideas and current limitations as well as suggest some new ways forward. Most of the article is focused on Quaternary volcanic systems of the continental crust, with comments about plutonic systems and a very little on the mantle.

2. WHAT CLOCKS ARE USED TO OBTAIN TIME INFORMATION FROM ROCKS?

There are two main approaches to access time information from rocks and minerals. One is based on the rate of radioactive decay and makes possible direct dating and absolute age determinations.

The other is based on thermodynamic and kinetic laws of equilibration of chemical heterogeneities and yields relative time information.

2.1. The Radioactive Timescale

The age determination of crystals or rocks is based on radioactive decay laws (formulated by Rutherford and Soddy in 1902). The nucleus of an unstable radioactive element (**N**), the so-called parent, spontaneously decays (→) with time (**t**) to a radiogenic nuclide so-called daughter ($\mathbf{N}_1^*$), so that $\mathbf{N} \rightarrow \mathbf{N}_1^*$ at a rate that is described by a decay constant (λ):

$$-\frac{\mathrm{d}\mathbf{N}}{\mathrm{d}\mathbf{t}} = \lambda \mathbf{N}. \quad 1.$$

Commonly used systems for age determination from magmatic rocks are $^{40}\mathrm{K} \rightarrow {}^{40}\mathrm{Ar}$ and $^{238}\mathrm{U} \rightarrow {}^{206}\mathrm{Pb}$ (e.g., Allègre 2008). The number of daughter isotopes present at a given time is $\mathbf{N}_1 = \mathbf{N}_1^* + \mathbf{N}_1^0$, where $\mathbf{N}_1^0$ is the number of daughter isotopes present initially, at time 0. With measurements of the parent and daughter isotopes, knowledge of the decay constant, and some constraints on the initial concentration of the daughter isotope, it is possible to obtain an age (e.g., Allègre 2008). A critical aspect is to have good constraints on the initial daughter isotope ($\mathbf{N}_1^0$), which is a priori unknown but is commonly addressed using the so-called isochron equation. Measuring the isotopic composition of more than one mineral (or crystal or rock), and assuming they have the same age and initial isotopic composition, it is possible to obtain the isochron age (e.g., Allègre 2008, Reiners et al. 2018):

$$\mathbf{N}_1 = \mathbf{N}_1^0 + \mathbf{N}\left(e^{\lambda \mathbf{t}} - 1\right). \quad 2.$$

To obtain a robust isochron age, at least three independent isotope determinations from cogenetic crystals or rocks are necessary. However, this is not possible in many situations, and two data points, pseudoisochrons, or model ages are used—for example, when dating volcanic rocks using zircon and glass (e.g., Cooper 2015, Reid et al. 1997). This may introduce some errors, but greater uncertainty arises when mineral separates with thousands of grains of potentially different ages are analyzed together and then used as a single analysis in the isochron diagram (e.g., Allègre 2008). The analysis of multigrains is necessary due to the low concentrations of many of the isotopes. In addition, one also needs to consider whether the mineral(s) or rock(s) have remained closed to additions or losses of parent or/and daughter atoms. Such modifications can occur due to weathering, radiation damage, and other post-crystallization processes. But they also arise due to the kinetic properties of elements—namely, different elements have different diffusion rates through the crystal lattice. In practical terms, the age is related to the so-called closure temperature, which is explained below in some detail (**Figure 3**).

Many geochronological studies have found that the ages obtained by U–Pb in zircon are typically tens to hundreds of thousands of years older than those obtained using $^{40}\mathrm{Ar}/^{39}\mathrm{Ar}$ of rock-forming silicates for the same samples (e.g., Costa 2008, Reid 2003). The $^{40}\mathrm{Ar}/^{39}\mathrm{Ar}$ system in volcanic rocks gives ages that are close to eruption when magma is quickly quenched (although see Andersen et al. 2017), and for plutonic rocks, the ages may be closer to or below the solidus of the magma. More specifically, all ages depend on the closure temperature ($\mathbf{T_c}$) of the mineral and the radiogenic daughter isotope according to (Dodson 1973) (**Figure 3**),

$$\frac{\mathbf{E}}{\mathbf{R}\mathbf{T_c}} = \ln\left(-\frac{\mathbf{A}\,\mathbf{D_o}\,\mathbf{R}\,\mathbf{T_c^2}}{\mathbf{E}\,\mathbf{s}\,\mathbf{a}^2}\right), \quad 3.$$

where **E** is the activation energy for volume diffusion, **R** is the gas constant, $\mathbf{D_o}$ is the pre-exponential factor of the diffusion coefficient (**D**), **A** is a geometric factor, **s** is the cooling rate,

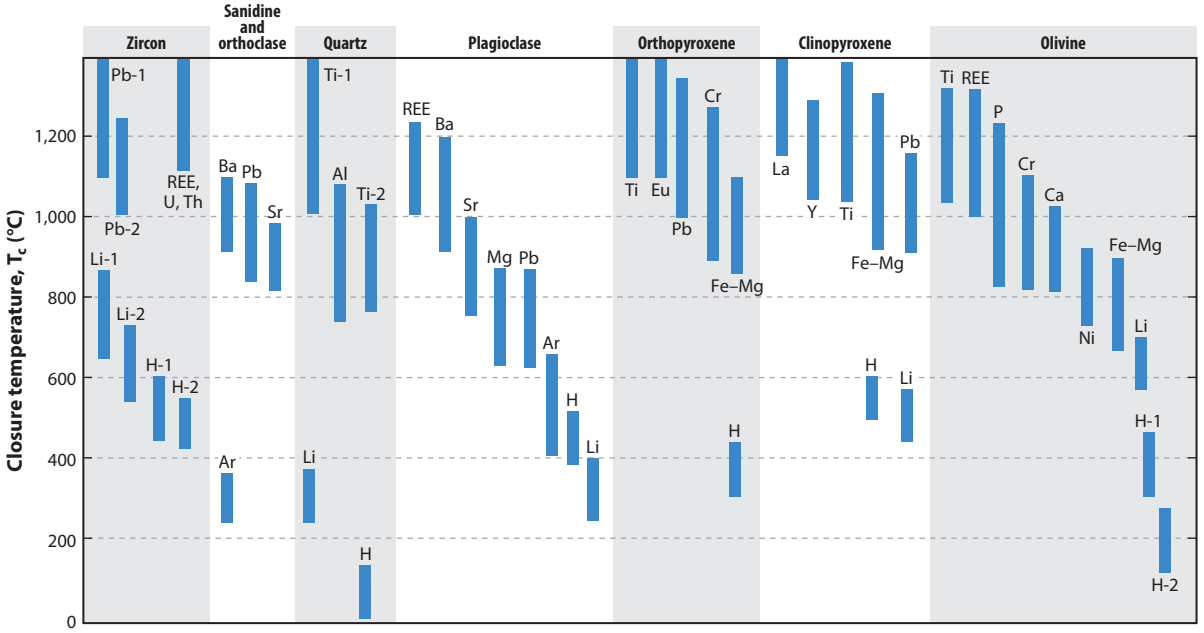

Figure 3

Closure temperatures for a range of elements calculated using Equation 3 and shown in the **Supplemental Spreadsheet**. The wide range of closure temperatures of different elements even in a single mineral has the potential to tightly constrain the temperature-time relations of magmatic systems. The elements and minerals shown illustrate the range of temperatures that can be explored but do not exhaustively cover all the data available in the literature. The closure temperatures are for a sphere of a radius of 250 μm (except where indicated for zircon, see below) and cooling rates between 1 and 10^{-3} °C/year. Abbreviation: REE, rare earth element. Data for olivine (*D* values are typically for forsterite = 90 and parallel to *c* axis): H-2 from Barth et al. (2019), Ti from Cherniak & Liang (2014), REE from Cherniak (2010) and Cherniak & Van Orman (2014), Ca from Coogan et al. (2005a), H-1 from Demouchy & Mackwell (2006), Fe–Mg from Dohmen & Chakraborty (2007), Li from Dohmen et al. (2010), Cr from Ito & Ganguly (2006), Ni from Petry et al. (2004), and P from Watson et al. (2015). Data for plagioclase (mostly labradorite): Pb from Cherniak (1995), Sr from Cherniak & Watson (1994), Ba from Cherniak (2002), REE from Cherniak (2003), Li from Giletti & Shanahan (1997), H from Johnson & Rossman (2013), Mg from Van Orman et al. (2014), and Ar from Wartho et al. (2013). Data for sanidine and orthoclase: Pb from Cherniak (1995), Sr from Cherniak (1996), Ba from Cherniak (2002), and Ar from Foland (1994). Data for clinopyroxene: Pb from Cherniak (1998, 2001), Ti from Cherniak & Liang (2012), Li from Coogan et al. (2005b), Fe–Mg from Müller et al. (2013), H from Sundvall et al. (2009), and La and Y from Van Orman et al. (2001). Data for orthopyroxene: Pb from Cherniak (2001), Eu from Cherniak & Liang (2007), Fe–Mg from Dohmen et al. (2016), Cr from Ganguly et al. (2007), H from Stalder & Skogby (2003), and Ti from Cherniak & Liang (2012). Data for quartz: Ti-2 from Cherniak et al. (2007), Ti-1 from Jollands et al. (2020), H from Kronenberg et al. (1986), Al from Tailby et al. (2018), and Li from Verhoogen (1952). Data for zircon (the 1 next to the element is for a crystal size of 100 μm, and the 2 is for 10 μm): Pb from Cherniak & Watson (2001); REE, U, and Th from Cherniak et al. (1997); H from Ingrin & Peipei (2016), and Li from Trail et al. (2016).

and **a** is the diffusing distance. The closure temperature expresses the condition at which a given crystal becomes closed to exchange of the daughter isotope with the environment via volume diffusion. All other parameters being equal, the daughter elements with the fastest diffusivities have the lowest closure temperatures (**Figure 3**; **Supplemental Spreadsheet**). Thus, it can partly explain why the U–Pb ages of zircons are older than $^{40}Ar/^{39}Ar$ in feldspars (e.g., Costa 2008, Reid 2003), although other factors may be equally important, as argued in Section 3.2. The development of thermochronology (Reiners et al. 2018) has exploited the range of closure temperatures and enabled scientists to track the thermal evolution of metamorphic rocks (e.g., Ganguly 2002, Kohn & Penniston-Dorland 2017), which is conceptually similar to understanding the thermal evolution of the magmatic systems discussed in this review.

Supplemental Material >

Table 1 Summary of the main attributes, time ranges, uncertainties, and materials used for obtaining time information from isotopes of U-series disequilibria

Parent → daughter	Half-life of the daughter (years)	Secular equilibrium (years)	Useful timescale (years)	Relative precision (%)	Sample requirements
$^{238}U \rightarrow {}^{230}Th$	75,690	400 k	1–400 k	>2	zircon, allanite, in situ analysis
				>0.1	zircon, allanite, single crystal
				1–10	silicates/WR, many grains[a]
$^{230}Th \rightarrow {}^{226}Ra$	1,599	8 k	100–10 k	1–10	silicates/WR, many grains[a]
$^{226}Ra \rightarrow {}^{210}Pb$	22.6	100	1–100	1–10	silicates/WR, many grains[a]

[a]Many grains means hundreds or thousands.

The time ranges, precisions, and sample requirements are approximations and depend on the exact sample and instrument used. Abbreviation: WR, whole rock. Data from Cooper (2015), Cooper & Reid (2008), Schmitt (2011), and Schmitt & Vazquez (2017).

2.1.1. U–Th-series disequilibria. The absolute precision of the dates decreases as the absolute time increases, and thus one can better determine the timescales of the shortest magmatic processes in younger rather than in older rocks (e.g., Allègre 2008). Dating of zircon with $^{238}U \rightarrow {}^{206}Pb$ can provide age information from magmatic systems with relative precisions as good as 0.1% and absolute precisions of a few thousand years (e.g., Schaltegger & Davies 2017). Even shorter timescales, especially from young volcanic rocks, can be obtained by applying the so-called U-series disequilibria, which include the radioactive chain of $^{238}U \rightarrow {}^{230}Th \rightarrow {}^{226}Ra \rightarrow {}^{210}Pb$ (e.g., Allègre 2008, Condomines et al. 2003, Reiners et al. 2018). This method requires the same conditions as noted above, except that the daughter isotope is also radioactive, and the initial condition is that of secular equilibrium. The concentrations of nuclides of the radioactive series are in secular equilibrium when the time is about 5 times the half-life of the daughter isotope (Condomines et al. 2003, Cooper & Reid 2008) (**Table 1**). A magmatic process that fractionates the parent-daughter nuclides such as partial melting, crystallization, or melt degassing (depending on the crystal-melt or melt-fluid partition coefficients) breaks the secular equilibrium concentration of the nuclides and starts the clock (Condomines et al. 2003, Cooper & Reid 2008). Using the full spectra of U-series isotopes allows one to determine times ranging from a few weeks to hundreds of thousands of years, depending on which process fractionates which element (**Figure 4**).

Dates from areas of tens of micrometers can be obtained with $^{238}U \rightarrow {}^{230}Th$ in accessory U-rich minerals such as zircon or allanite using an in situ method, such as the ion microprobe [secondary-ion mass spectrometry (SIMS)] or laser ablation inductively coupled plasma mass spectrometry (LA-ICP-MS) (e.g., Schmitt 2011, Schmitt & Vazquez 2017). However, the low concentrations of the relevant isotopes in rock-forming silicates cannot be obtained using in situ methods and require the use of mineral separates of hundreds or thousands of grains, which likely include crystals of different ages (e.g., **Figure 2**); thus, these ages are likely of mixed crystal populations. Moreover, the presence of accessory minerals and melt inclusions in the rock-forming minerals needs to be accounted for, as they concentrate the relevant isotopes and thus add significant uncertainty to interpretation of the ages of the rock-forming minerals (e.g., Cooper 2015, Cooper & Reid 2008).

One advantage of U-series disequilibria dating is that a single measurement can place boundaries on the time between the parent-daughter fractionation event and eruption. This has been

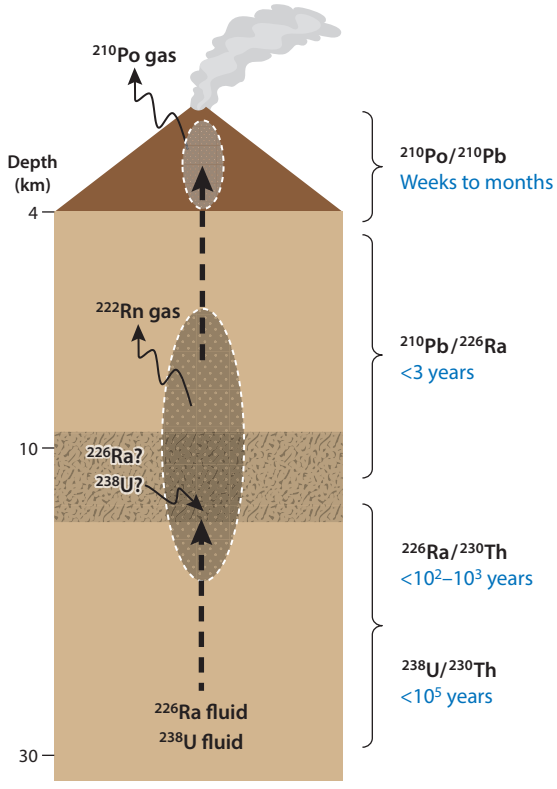

Figure 4

Schematic representation of a volcano plumbing system and the ranges of times and types of processes that can be obtained via U-series disequilibria methods. Note the large range of timescales that can be obtained and that different parent-daughter systems record the timescales of different processes, from volatile loss from the melt to crystal-liquid separation. ^{226}Ra and ^{238}U excesses on timescales less than 8,000 years and less than 380,000 years, respectively, can be generated by fluid addition from a subducting slab. Crustal assimilation of carbonate material can potentially contribute the addition of ^{226}Ra and ^{238}U to the magma; ^{222}Rn and ^{210}Po can track the much shorter timescale of magma ascent and degassing of volatile-rich magma. Figure and caption adapted with permission from Handley et al. (2018), figure 6, for Merapi volcano.

successfully used to obtain maximum eruption ages (e.g., Condomines et al. 2003, Sims et al. 2013). Moreover, U-series data can also be used to determine the timescales of mantle melting and transport toward the surface, magmatic differentiation of cogenetic rock associations, and melt degassing (e.g., Condomines et al. 2003, Dosseto et al. 2010) (**Figure 4**).

2.2. The Thermodynamic Timescale

Diffusion chronometry is another approach to obtain time information, and it is based on irreversible thermodynamics and kinetic laws (e.g., Costa & Morgan 2010, Costa et al. 2008). The second law of thermodynamics states that the entropy of an isolated system increases with time, which has been dubbed time's arrow because it gives a direction to processes that could otherwise be time reversible (e.g., Richet 1999). In practical terms, time can be obtained from the conditions of chemical equilibrium and application of Fick's laws. Fick's second law in one dimension (**x**, distance) relates the change of concentration (**C**) with time (**t**) to the change of gradient of

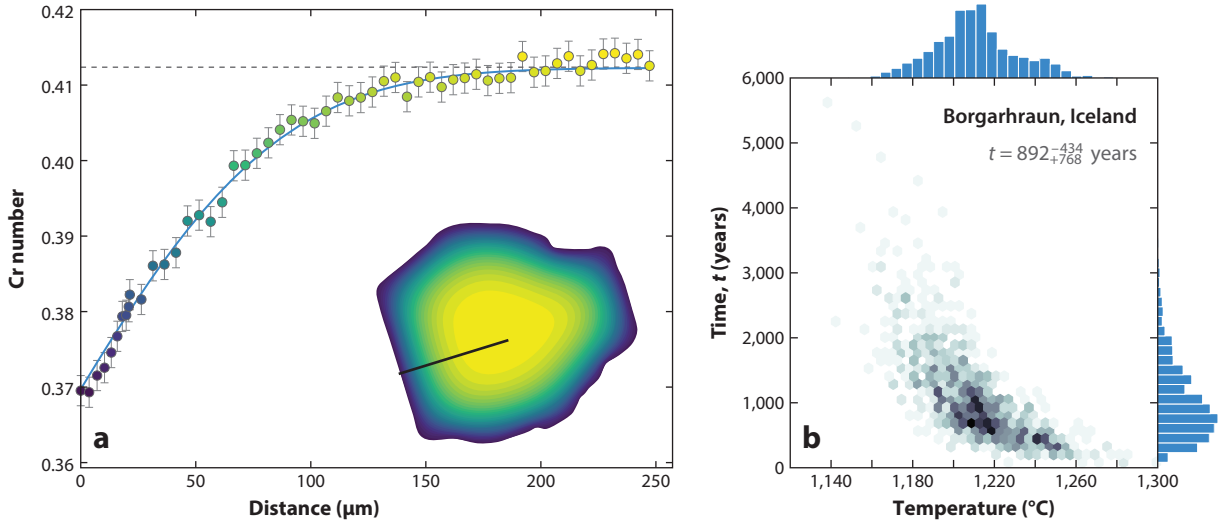

Figure 5

Example of determination of timescales of magmatic processes from zoning patterns of crystals. (*a*) The crystal is a spinel zoned in Cr for which one can obtain a two-dimensional map of the chemical distribution (*inset*) and a one-dimensional profile that has been fitted to obtain a time. The model reproduces the data quite well. The dashed gray line is the assumed initial concentration distribution, and the boundary has been assumed to be constant with time and equal to that of the outermost rim. (*b*) The times obtained vary depending on the temperature. Mutch et al. (2019) used a Bayesian approach to estimate the error of the time and report the median and 1 σ. The time in this example illustrates a magma mixing event that occurred in the lower crust for the Borgarhraun eruption in Iceland. Figure adapted with permission from Mutch et al. (2019).

concentration, and the diffusion coefficient (**D**):

$$\frac{\partial \mathbf{C}}{\partial \mathbf{t}} = \mathbf{D}\frac{\partial^2 \mathbf{C}}{\partial \mathbf{x}^2}. \quad 4.$$

To obtain a time, one solves this equation by numerical methods (e.g., finite differences) or an analytical solution (Crank 1975), depending on the initial (e.g., concentration distribution at time 0 for all **x**) and boundary conditions. The latter include whether the system is finite and whether the concentration at the boundaries is constant with time. With a given set of conditions, measurement of concentration gradients in minerals or glass, and knowledge of the diffusion coefficient, one can solve for time using a forward model (e.g., Costa & Morgan 2010, Costa et al. 2008, Girona & Costa 2013) (**Figure 5**).

The power of this approach is that many time determinations can be obtained from a single sample using multiple elements in a single crystal (e.g., Costa & Dungan 2005), a range of minerals (e.g., Chamberlain et al. 2014, Fabbro et al. 2017), and many crystals (tens to hundreds) (Pankhurst et al. 2018). Moreover, the wide range of spatial scales (from tens of nanometers to hundreds of micrometers), the improved precision with which elements and isotopes can be measured nowadays (e.g., by LA-ICP-MS, SIMS, nanoscale SIMS, and atom probe tomography) (Cao et al. 2019, Manzini et al. 2017, Oeser et al. 2015, Till et al. 2015), and the wide range of closure temperatures (**Figure 3**) make it possible to access timescales of a few seconds to millions of years (e.g., Costa et al. 2020). The precision of the time determination does not depend on the absolute age, and thus very short timescales can be obtained for very old samples.

The large potential of the kinetic approach is, however, tempered by the uncertainties involved in the times that are obtained. Some uncertainties are related to the natural system, including the spatial and analytical precision of the concentration profile, the goodness of the model fit, how well

one knows the temperature and initial and boundary conditions, the effect of crystal growth and dissolution, and the effect of two- and three-dimensional diffusion. Except for the temperature, the uncertainty in most of these variables is typically less than 50% and can be greatly minimized by careful petrological observations and multielement analysis as reported in detail elsewhere (e.g., Costa & Morgan 2010; Costa et al. 2008; Flaherty et al. 2018; Gualda et al. 2012; Shea et al. 2015a,b).

The largest uncertainties are related to the temperature and the accuracy/precision of the diffusion coefficient. These two factors are combined in the Arrhenius-type dependence of the diffusion coefficient on temperature:

$$\mathbf{D} = \mathbf{D_o}\ \exp\left(-\frac{\mathbf{E}}{\mathbf{R}\,\mathbf{T}}\right). \qquad 5.$$

The diffusion coefficient also depends on pressure (although it can typically be ignored for crustal pressures), whose effect is included in the exponential (e.g., Chakraborty 2010). Diffusion of some elements also depends on the mineral composition itself, the oxygen and water fugacities, with these effects typically included in the pre-exponential factor (e.g., for Fe–Mg in olivine, see Dohmen & Chakraborty 2007). The contribution of these parameters to the value of the diffusion coefficient is typically smaller than that of temperature (e.g., Zhang & Cherniak 2010).

Errors associated with temperature and the experimentally calibrated values of $\mathbf{D_o}$ and $\mathbf{E}$ can be quite variable and depend on the natural system and the experimental study. Temperature uncertainties from natural systems vary from about 10°C if experimental phase equilibria are used to about 50°C for many geothermometers (e.g., Putirka 2008). The combined effect of uncertainties in $\mathbf{T}$, $\mathbf{E}$, and $\mathbf{D_o}$ on the value of $\mathbf{D}$ can be calculated by error propagation of Equation 5 (e.g., Gualda et al. 2012) (**Supplemental Text**). The errors on $\mathbf{D}$ can be quite variable, from about 70% to 350% (or much larger), and these are directly translated into the error of the calculated times (**Table 2**). However, with these uncertainties, it is still possible to distinguish between various magmatic hypotheses, and for some applications one is interested in relative time differences, and thus the uncertainty when comparing times using the same mineral/element is not as significant.

Supplemental Material >

3. MAIN FINDINGS AND HYPOTHESES ABOUT MAGMATIC SYSTEMS FROM AGE AND TIMESCALE STUDIES

Studies that investigate the rates and timescales of magmatic systems can be loosely grouped into those that focus on relatively small mafic eruptions (less than 1 km^3) and those aiming at understanding processes related to large silicic magma bodies (greater than 10 km^3). Selected examples that illustrate the findings and problems of both types of studies are described below.

3.1. Timescales of Magma Replenishment, Mixing, Differentiation, and Degassing

Many studies have used diffusion chronometry to quantify the timescales of arrival of mafic magma in shallow reservoirs and have found times that vary from a few weeks to a few years (e.g., Costa et al. 2020). These times are similar to the eruption frequencies of many of these volcanoes (e.g., Etna, Stromboli, Piton de la Fournaise, Kilauea), which implies that many eruptions are driven by magma replenishment, that most intruded magma is erupted, and thus that the volcanic system is in a steady state, as has also been inferred by time-series analysis of geochemical data (Albarède 1993). Other studies highlight the importance of crystal-rich plumbing systems, as crystals contain resorbed cores that belong to earlier intrusions (decades to hundreds of years) and rims that record

Table 2 Examples of magnitude error in the diffusion coefficient associated with the uncertainties (1 σ) of experimentally calibrated values of the pre-exponential factor of the diffusion coefficient (D_o) and the activation energy for volume diffusion (E), and assuming a temperature (T) uncertainty from the natural system of 25°C

Element, mineral	D_o (m^2s^{-1})	D_o (m^2s^{-1}) 1 σ	E ($kJmol^{-1}$)	E ($kJmol^{-1}$) 1 σ	T (°C)	T (°C) 1 σ	D (m^2s^{-1})	D (m^2s^{-1}) 1 σ	F	%
Ni, olivine	3.84×10^{-9}	$+2.50 \times 10^{-9}$, -1.50×10^{-9}	216	6	1,150	25	4.52×10^{-17}	$+4.00 \times 10^{-17}$, -3.24×10^{-17}	0.9, 0.7	90, 70
Sr, plagioclase	1.78×10^{-7}	$+3.80 \times 10^{-7}$, -8.32×10^{-8}	265	8	950	25	8.54×10^{-1}	$+2.00 \times 10^{-18}$, -9.04×10^{-19}	2.3, 1.1	230, 110
Fe–Mg, clinopyroxene	2.77×10^{-7}	$+8.76 \times 10^{-7}$, -8.76×10^{-8}	230	16	1,050	25	6.03×10^{-20}	$+2.12 \times 10^{-19}$, -9.57×10^{-20}	3.5, 1.6	350, 160
Ti, quartz	5.01×10^{-9}	$+1.26 \times 10^{-8}$, -2.00×10^{-9}	311	12	750	25	6.60×10^{-25}	$+1.99 \times 10^{-24}$, -1.13×10^{-24}	3.0, 1.7	300, 170

Error in **D** calculated by error propagation assuming independent errors (see **Supplemental Text**). Note that errors in **D** are not symmetrical because $\mathbf{D_o}$ and **E** are typically obtained by linear regression of Log of Equation 5 (e.g., $\ln\mathbf{D} = \ln\mathbf{D_o} - [\mathbf{E/RT}]$). These numbers are the percent of the contribution to the error in **D** from $\mathbf{D_o}$, **E**, and **T**. **F** is the factor error and translates directly to a factor in the timescale. For example, if time calculated from Ni was 100 days, it would read 100^{+90}_{-70} days. Also shown is the relative error in percent. Data for Ni in olivine from Petry et al. (2004), for Sr in plagioclase from Cherniak & Watson (1994), for Fe–Mg in clinopyroxene from Müller et al. (2013), and for Ti in quartz from Jollands et al. (2020).

much shorter times (e.g., Di Stefano et al. 2020, Ubide et al. 2019). Crystals from monogenetic or/and dike-fed eruptions record magma transport and storage times of weeks to months (e.g., Albert et al. 2020, Brenna et al. 2018, Pankhurst et al. 2018, Ruprecht & Plank 2013), whereas magma mixing in the lower crust has been reported to occur over several centuries before eruption (e.g., Mutch et al. 2019).

The timescale data from these studies can be used to establish an absolute time series of events of magmatic processes if the eruption dates are known (Kahl et al. 2011). It has thus become possible to track magma storage changes with time as the system gets closer to eruption and relate these to volcano monitoring data sets (e.g., Albert et al. 2019, Costa et al. 2020, Kahl et al. 2013, Rasmussen et al. 2018, Ruth et al. 2018). One example is the 2010 flank eruption of Eyjafjallajökull volcano (Pankhurst et al. 2018) (**Figure 6**). The absolute times and distributions obtained from the crystals indicate magma intrusion and stalling at shallow depth and a cumulative number of earthquakes, and they match quite well with the timing and relative magnitude changes of the GPS displacements (**Figure 6**). This suggests a cause-effect relationship between the magmatic processes at depth and the monitoring signals at the surface, which is a step forward toward more robust conceptual models involved in eruptions at these volcanoes.

The timescales of the shallow processes described above are typically too short to be obtained using U-series disequilibria on single crystals or zones of crystals (e.g., Cooper 2015). However, analysis of historical sequences of lavas, and glass-rich samples, combined with geochemical modeling has provided insights into the timescale of magma differentiation and degassing (e.g., Condomines et al. 2003). For example, Sigmarsson (1996) used ^{210}Pb–^{226}Ra disequilibria in Surtsey and Heimaey (Iceland) lavas to infer a time of about 10 years for a small volume of basaltic magma to differentiate into hawaiite and mugearite magmas. More recently, Bragagni et al. (2014) investigated the ^{230}Th/^{232}Th changes over two decades of Stromboli volcanic eruptions and

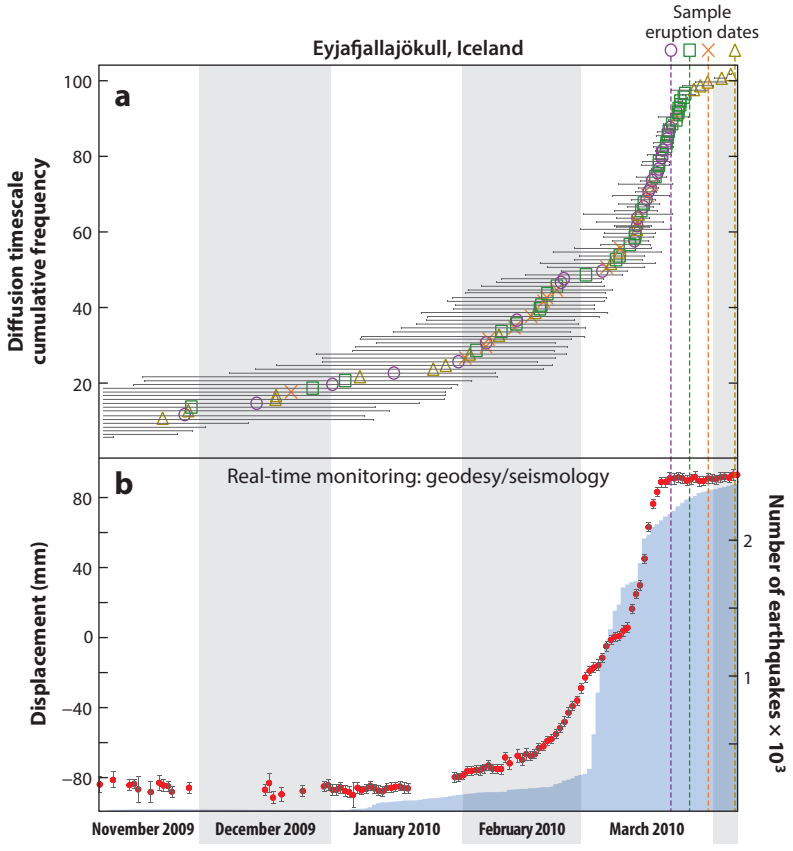

Figure 6

Example of the relationship between the timescales obtained from crystals and those of monitoring networks. (*a*) Timescale information distribution from the olivine crystals of the 2010 flank eruption of Eyjafjallajökull volcano where the relative times for magma crystallization and setting in a dike have been recalculated to absolute time and plotted in a cumulative form. They show a distribution that is close to exponential, with an increasing amount of times as the system gets closer to eruption. (*b*) Time series of monitoring data for ground displacement (GPS SKOG station, *red circles with error bars*) and cumulative number of earthquakes (from Sigmundsson et al. 2010). The good correlation in time and cumulative distributions of the crystal and monitoring data indicate the data from crystals are recording the processes that are occurring at depth and that are recorded as monitoring signals on the surface. In this case one can see magma intrusion, crystallization, and movement toward the surface. Figure adapted with permission from Pankhurst et al. (2018), figures 5 and 8.

inferred magma residence times of a few years to about half a century. Finally, Handley et al. (2018) investigated multiple samples from the 2006 and 2010 eruptions of Merapi volcano and were able to use the very short-lived $^{210}Po/^{210}Pb$ disequilibria to infer the timescales of magma degassing of a few months, in accordance with those monitored at the surface (**Figure 4**).

3.2. Growth and Storage of Large Silicic Magma Reservoirs

The timescales and magmatic processes related to large silicic eruptions and plutons (greater than 100 km^3) have been mainly obtained using single zircon crystals. Many studies have found that the

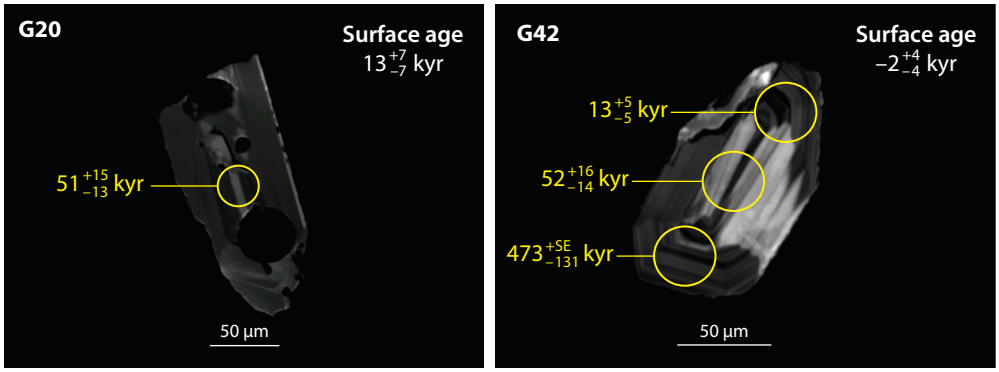

Figure 7

Cathodoluminescence images of two zircon crystals (G20 and G42) with examples of ranges of ages that can be obtained from different zones of a single zircon crystal using in situ methods. Note that it is possible to determine the age of the outermost crystal rim, and that in some cases it overlaps with that of eruption (G42), but in other cases it can be much older. The large range of ages within a single crystal records the complex history of magma accumulation over tens of thousands of years and which likely involve large thermal fluctuations from close to the solidus to the liquidus. Figure adapted with permission from Rubin et al. (2017).

zircon ages are tens to hundreds of thousands of years older than eruption age, or even longer for times between crystallization, growth, and solidification of plutonic complexes (e.g., Costa 2008, Reid 2003, Schaltegger & Davies 2017). Such long time spans have also been recorded within a single crystal using in situ methods (**Figure 7**). The zircon age data are interpreted to reflect the processes involved in the buildup and storage of these large amounts of magma. The long residence times were initially obtained from Rb–Sr isochrons of feldspars for the Long Valley caldera system (Halliday et al. 1989) and later by in situ zircon data (Reid et al. 1997). They were taken as evidence for the existence of large and liquid-dominated upper crustal magma chambers (e.g., Halliday et al. 1989), although already Mahood & Halliday (1990) argued that parts of the reservoir could be frozen as an immobile mush that could be defrosted before eruption. This interpretation is similar to more recently proposed views that reservoirs are crystal rich and are built over tens of thousands of years or longer by smaller incremental additions of magma (e.g., Cooper 2015, Cooper & Kent 2014, Wilson & Charlier 2009). Incremental addition of magma batches has also become the new working hypothesis for the buildup of large plutons (Barboni et al. 2015, Coleman et al. 2004, Miller et al. 2007, Schoene et al. 2012).

A key component for understanding the meaning of these crystal ages is the diffusion chronometry timescales. Diffusion chronometry results from pyroxenes, quartz, and feldspars (e.g., Allan et al. 2013, Chamberlain et al. 2014, Druitt et al. 2012, Fabbro et al. 2017, Gualda et al. 2012, Till et al. 2015) vary from a few years to a few hundred years (rarely up to 1 kyr) and thus are much shorter than those obtained from zircon ages. Such a time difference has generated a range of hypotheses about the magmatic system (**Figure 8**). One interpretation is that the rock-forming silicates mainly record the last thermal or/and compositional perturbation of the system (e.g., Turner & Costa 2007). A further possibility is that the zircon and the rock-forming minerals actually grew at different times (e.g., Reid 2003). Zircon dissolves more slowly in silicate melts than most rock-forming minerals (e.g., Zhang 2008); it can survive multiple reheating episodes.

An interpretation that has attracted much attention is that the magmatic system may spend a significant amount of time below the closure temperature of most elements and rock-forming minerals (**Figure 3**), and thus the diffusion clock could effectively stop (e.g., Cooper & Kent 2014). This hypothesis has been called cold storage and has been contrasted with the alternative warm

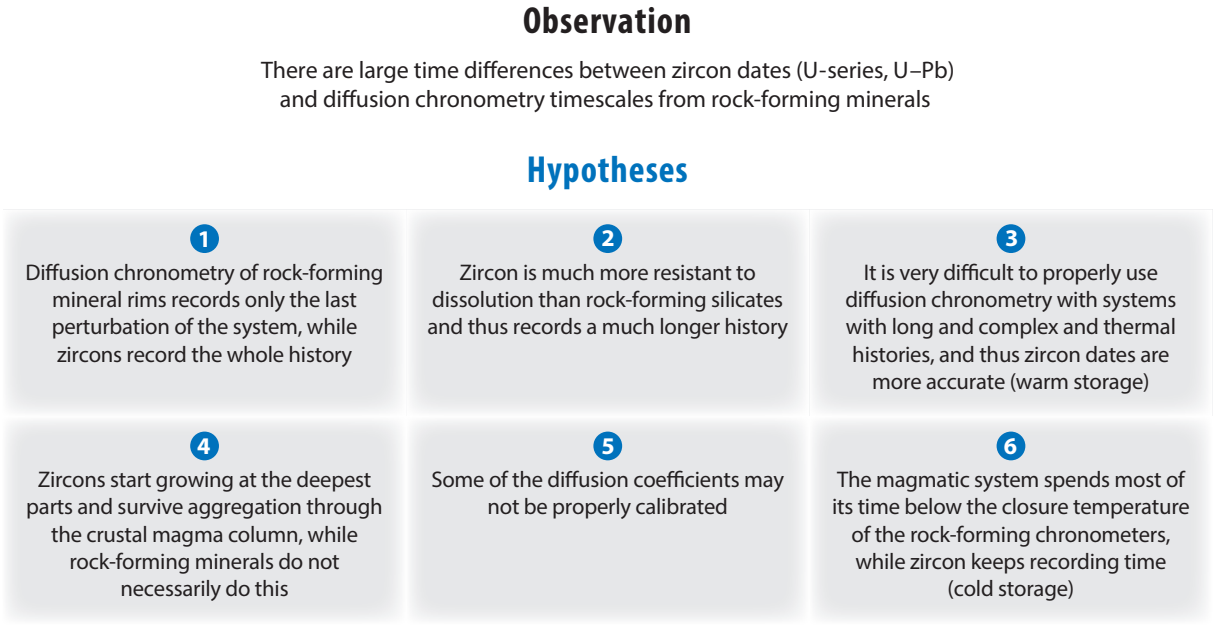

Figure 8

Nonexhaustive and nonexclusive list of hypotheses that have been put forward (and are discussed in the text) to interpret the difference between zircon (and allanite) radiometric dates and times obtained from diffusion chronometry for the same system. Distinguishing between the different possibilities requires a comprehensive study of the magmatic system at hand, from using diffusion chronometry of rock-forming minerals to in situ dating of accessory minerals. Moreover, the errors of some of the time determinations and the representativeness of the limited number of crystals that can be studied also need to be considered for a more robust interpretation.

storage, where the zircon time and temperature relations indicate continued storage at a high temperature for hundreds of thousands of years, which would be difficult to capture by diffusion chronometry studies (e.g., Barboni et al. 2016, Miller 2016). Finally, some studies of plutonic rocks suggest that zircon could have crystallized at deep crustal levels and was subsequently transported to the upper crust in small magma batches (e.g., Barboni et al. 2015, Schaltegger & Davies 2017).

Three studies have recently provided exceptional data sets that combine diffusion chronometry and mineral dating and have contributed to this debate in new ways. Rubin et al. (2017) obtained (for the first time) in situ zircon ages and diffusion chronometry times by modeling the zoning patterns of Li in the exact same materials. They found that the zircons recorded tens of thousands of years of crystallization, whereas the timescales for Li were of only a few decades. Given the low closure temperature of Li in zircon (**Figure 3**), this implies that the magma was stored at temperatures close to the solidus for long periods of time and thus supports the cold storage hypothesis. However, it is unclear whether the Li diffusivity is understood well enough to derive such conclusions (e.g., Cooper et al. 2017, Sliwinski et al. 2018, Tang et al. 2017, Wilson et al. 2017). The importance of properly understanding diffusion kinetics was recently exemplified by Jollands et al. (2020), who reported Ti diffusivity values in quartz that are about 100 times slower than those found by Cherniak et al. (2007). This new data set could imply that thermal fluctuations derived from Ti diffusion chronometry in quartz from silicic magmas such as the Bishop Tuff could last for tens of thousands of years, in agreement with (or even longer than) those obtained from zircon age data (e.g., Chamberlain et al. 2014, Gualda et al. 2012, Reid & Coath 2000, Simon & Reid 2005, Wark et al. 2007). This is consistent with a hot storage hypothesis (Jollands et al. 2020).

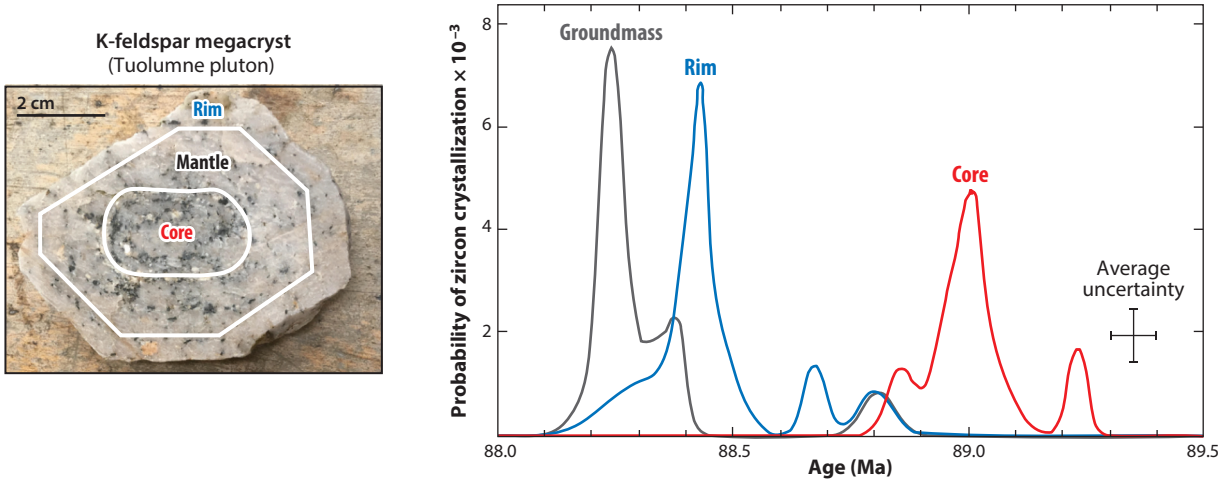

Figure 9

Example of the importance of obtaining crystal ages from zircons that are texturally controlled and placed into an overall context of the processes. Chambers et al. (2020) extracted zircon crystals from the core and rim of a K-feldspar megacryst, as well as from the matrix of the Tuolumne pluton (Yosemite National Park, USA). They found that the zircon crystals became progressively younger from the center to the rim and matrix. The finding implies that the megacryst was growing for about 500 kyr during which melt was present. Such data sets are critical to obtain more robust insights into the processes, as opposed to crushing up the whole rock and obtaining ages from zircons without textural context. Figure adapted with permission from Chambers et al. (2020), figures 2 and 3.

Finally, a plutonic perspective on these processes was recently provided by Chambers et al. (2020), who precisely dated zircons included in different parts of a large K-feldspar megacryst (greater than 3 cm) from the Tuolumne granitoid batholith. The zircons in the crystal core are about 500 kyr older than those in the rim, which are, in turn, older than those in the matrix (**Figure 9**). Thus, growth of this K-feldspar crystal spanned several hundred kiloyears and thus presumably also supports a hot storage scenario, although the errors in time determination still allow periods of a few hundred to a few thousand years of low temperature storage.

4. MAIN CHALLENGES AND POTENTIAL WAYS FORWARD

Despite the above-mentioned significant advances in revealing magmatic crystal ages, several limitations preclude more robust and quantitative understanding. Some of the limitations are related to precise dating of small parts of crystals by U–Th disequilibria, and others are linked to the errors associated to the diffusion chronometry times. There are also problems of sampling bias and representativeness of the crystals that are used to derive the time information. Below are some proposed avenues of research, and the reader is referred to additional suggestions by Cooper (2019) and Costa et al. (2020).

4.1. Improve the Robustness of Diffusion Chronometry Times with Integration of Information from Multiple Elements and Minerals and Better Constraints on Temperature

It is now possible to analyze a wide range of elements with a high spatial resolution and precision, which, when combined with the wide range of closure temperatures (**Figure 3**), affords a more realistic view of the temperature-time relations of a magmatic system. A few studies have used multielement and multimineral data sets, but analysis should be done more systematically

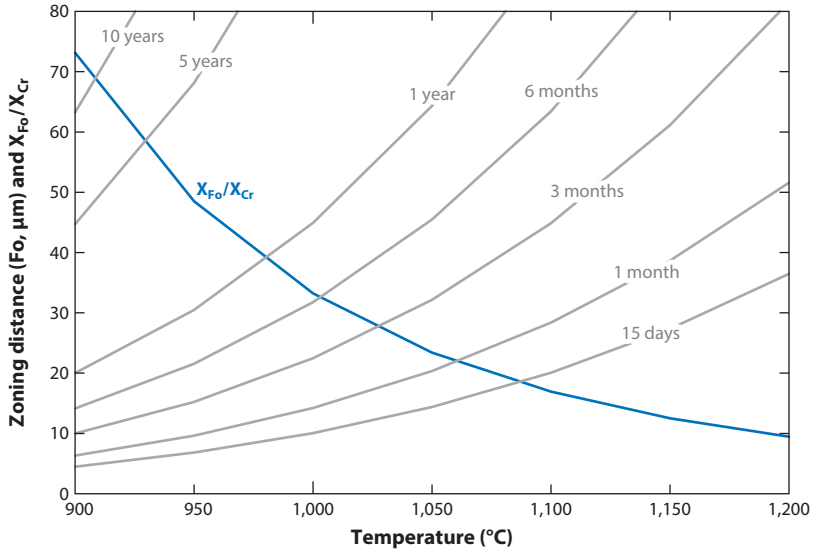

Figure 10

Example of the use of two elements with different activation energies [$\mathbf{X_{Fo}}$ is about 200 kJ/mol (Dohmen & Chakraborty 2007), and $\mathbf{X_{Cr}}$ is about 300 kJ/mol (Ito & Ganguly 2006)] that diffuse in the same mineral (olivine) to constrain simultaneously temperature and time. The blue curve shows how the ratio of the diffusion distance of the two elements varies with temperature, and it is independent of time. Measurement of such a ratio from a natural olivine can be used to obtain the temperature. Knowing the temperature, using the diffusion distance of one of the two elements (here shown for **Fo**) allows one to obtain the time. It is worth noting that these findings are valid only when the two elements have the same initial and boundary conditions and the solution for distance is for a homogenous initial condition and for semi-infinite media. Please see the main text for more details.

to explain the differences between the times obtained from different minerals and elements (e.g., Chamberlain et al. 2014, de Maisonneuve et al. 2016, Fabbro et al. 2017, Flaherty et al. 2018). An unexplored advantage of using multiple elements is that, in principle, it is possible to obtain both temperature and time simultaneously, and thus potentially decrease the error of the calculated times. If two elements (*i* and *j*) in the same crystal have significantly different activation energies ($\mathbf{E}_i \neq \mathbf{E}_j$) and have the same initial and boundary conditions, one can use (as an example) the relation for the characteristic diffusion distance as $\mathbf{x}^2 = \mathbf{D}^*\mathbf{t}$ and write the following equations:

$$\mathbf{x}_i^2 = \mathbf{D}_i\ (\mathbf{T})^*\,\mathbf{t}, \tag{6.}$$

$$\mathbf{x}_j^2 = \mathbf{D}_j\ (\mathbf{T})^*\,\mathbf{t}, \text{ and} \tag{7.}$$

$$\frac{\mathbf{x}_i^2}{\mathbf{x}_j^2} = \frac{\mathbf{D}_i\ (\mathbf{T})}{\mathbf{D}_j\ (\mathbf{T})}, \tag{8.}$$

where the dependence of **D** on **T** [$\mathbf{D}_i$ (**T**)] follows Arrhenius-type Equation 5. From Equation 8 it becomes apparent that the ratio of diffusivities of the two elements at the same temperature is equal to the ratio of the square root of their diffusion distances (**Figure 10**). Thus, by measuring the diffusion distances of the two elements in a natural crystal, one can find a unique **T** that is independent of time, and simple replacement of Equation 8 in Equations 6 or 7 gives the time. How well this approach can constrain temperature and time depends on the differences between

activation energies and diffusion distances, but it should be possible, for example, to use Fe–Mg and Cr diffusion in olivine (**Figure 10**). If diffusion anisotropy for the same element includes different activation energies, one can use a single element to get **T** and **t** (Cr in olivine) (Ito & Ganguly 2006). This approach could be expanded to different elements in different minerals as it is done in thermochronology (e.g., Reiners 2009), but additional assumptions are necessary on the initial plus boundary conditions.

4.2. Improve the Robustness of U–Th Age Dating and Times by Integrating Information from Multiple Decay Systems and Minerals with Textural Controls and Diffusion Chronometry

Most crystal age data derived from U-series disequilibria are from zircon or allanite, with comparatively few data sets from rock-forming minerals (e.g., Cooper 2015, 2019; Cooper & Reid 2008). This is because the much lower concentrations of the isotopes in the silicates do not allow for individual zones to be precisely analyzed and because of the need for many correction procedures when mineral separates are used (e.g., Cooper 2015). A very limited number of studies have dated accessory and major minerals in the same samples, and they seem to record different stages and/or locations of storage in the reservoir (Cooper 2015). There are also a limited number of cases where ^{238}U–^{230}Th ages and ^{230}Th–^{226}Ra ages have been measured in the same samples, and they give discordant apparent ages indicating multistage crystallization and/or mixing of multiple crystal populations (Reiners et al. 2018). More studies that combine accessory and major minerals and different isotopic systems in the same materials are necessary, but progress seems to depend on analytical advances in in situ mass spectrometry or perhaps on microdrilling of large crystals (e.g., Condomines et al. 2003). Combining detailed textural information with the ages of the analyzed accessory minerals (e.g., Kohn & Penniston-Dorland 2017) can also bring new insights (e.g., Chambers et al. 2020) (**Figure 9**). Finally, combining age dating and diffusion chronometry in the same minerals remains very challenging, but it seems a sure avenue for new discoveries to be made (e.g., Rubin et al. 2017).

4.3. Crystal Statistics and Integration of Physicochemical Models into Age Dating and Diffusion Chronometry

The meaningfulness of radiometric dates and time information depends on the availability, choice, and number of crystals that are studied. In both methods one is limited in the number of crystals, and given the variety of crystal textures and compositions in a single hand specimen (**Figure 2**), it is important to establish whether the studied crystals/samples are representative (e.g., Cheng et al. 2017). Moreover, it is also important to test whether the resolution of the crystal radiometric dates is adequate to test the hypothesis one is proposing, and thus more statistical analysis of the crystal populations and sampling bias effects is needed (e.g., Cheng et al. 2020, Kent & Cooper 2018).

Finally, coupling of thermal and chemical evolution models with crystal age and diffusion chronometry is currently one of the research frontiers. This is not easy, given the complexity of multiphase magmas (coupling of crystals, melt, and fluids), the multicomponent nature of silicate melts (thermodynamic and kinetic nonideality), the lack of diffusion data for many trace elements in the melt, and the wide ranges of physical properties of magmas and crystal-rich systems (e.g., Bachmann & Huber 2019, Bergantz et al. 2015). A few studies from plutonic systems have incorporated thermal modeling to the interpretation of their radiometric dating results (e.g., Barboni et al. 2015, Karakas et al. 2019). Likewise, a few studies using diffusion chronometry have addressed

the importance of realistic temperature and boundary changes during magma mixing (e.g., Cheng et al. 2020, de Maisonneuve et al. 2016). Finally, some progress has been made with the coupling of thermal evolution and crystallization and dissolution of zircon (Bindeman & Melnik 2016), but addition of silicates would make it possible, for example, to test whether the different timescales obtained from rock-forming minerals and zircons are due to differential dissolution rates (e.g., Zhang 2008).

DISCLOSURE STATEMENT

The author is not aware of any affiliations, memberships, funding, or financial holdings that might be perceived as affecting the objectivity of this review.

ACKNOWLEDGMENTS

F.C. thanks M. Chamber, V. Memeti, M. Pankhurst, E. Mutch, and K. Cooper for sharing the original figures of their papers; D. Ruth for the image in **Figure 2**; Y. Soon for help with **Figure 1** and advice on using Adobe for illustrations; D. Schonwalder for help in compiling diffusion data; and P. Adamek for suggestions with the English language. An anonymous reviewer provided useful comments. F.C. acknowledges a Singapore National Research Foundation Investigatorship award (grant number NRF-NRFI2017-06).

LITERATURE CITED

Albarède F. 1993. Residence time analysis of geochemical fluctuations in volcanic series. *Geochim. Cosmochim. Acta* 57(3):615–21

Albert H, Costa F, Di Muro A, Herrin J, Métrich N, Deloule E. 2019. Magma interactions, crystal mush formation, timescales, and unrest during caldera collapse and lateral eruption at ocean island basaltic volcanoes (Piton de la Fournaise, La Réunion). *Earth Planet. Sci. Lett.* 515:187–99

Albert H, Larrea P, Costa F, Widom E, Siebe C. 2020. Crystals reveal magma convection and melt transport in dyke-fed eruptions. *Sci. Rep.* 10(1):11632

Allan ASR, Morgan DJ, Wilson CJN, Millet MA. 2013. From mush to eruption in centuries: assembly of the super-sized Oruanui magma body. *Contrib. Mineral. Petrol.* 166(1):143–64

Allègre C. 2008. *Isotope Geology*. Cambridge, UK: Cambridge Univ. Press

Andersen NL, Jicha BR, Singer BS, Hildreth W. 2017. Incremental heating of Bishop Tuff sanidine reveals preeruptive radiogenic Ar and rapid remobilization from cold storage. *PNAS* 114(47):12407–12

Bachmann O, Huber C. 2019. The inner workings of crustal distillation columns; the physical mechanisms and rates controlling phase separation in silicic magma reservoirs. *J. Petrol.* 60(1):3–18

Bacon CR, Lowenstern JB. 2005. Late Pleistocene granodiorite source for recycled zircon and phenocrysts in rhyodacite lava at Crater Lake, Oregon. *Earth Planet. Sci. Lett.* 233(3–4):277–93

Barboni M, Annen C, Schoene B. 2015. Evaluating the construction and evolution of upper crustal magma reservoirs with coupled U/Pb zircon geochronology and thermal modeling: a case study from the Mt. Capanne pluton (Elba, Italy). *Earth Planet. Sci. Lett.* 432:436–48

Barboni M, Boehnke P, Schmitt AK, Harrison TM, Shane P, et al. 2016. Warm storage for arc magmas. *PNAS* 113(49):13959–64

Barth A, Newcombe M, Plank T, Gonnermann H, Hajimirza S, et al. 2019. Magma decompression rate correlates with explosivity at basaltic volcanoes—constraints from water diffusion in olivine. *J. Volcanol. Geotherm. Res.* 387:106664

Bergantz GW, Schleicher JM, Burgisser A. 2015. Open-system dynamics and mixing in magma mushes. *Nat. Geosci.* 8(10):793–96

Bindeman IN, Melnik OE. 2016. Zircon survival, rebirth and recycling during crustal melting, magma crystallization, and mixing based on numerical modelling. *J. Petrol.* 57(3):437–60

Bragagni A, Avanzinelli R, Freymuth H, Francalanci L. 2014. Recycling of crystal mush-derived melts and short magma residence times revealed by U-series disequilibria at Stromboli volcano. *Earth Planet. Sci. Lett.* 404:206–19

Brenna M, Cronin SJ, Smith IEM, Tollan PME, Scott JM, et al. 2018. Olivine xenocryst diffusion reveals rapid monogenetic basaltic magma ascent following complex storage at Pupuke Maar, Auckland Volcanic Field, New Zealand. *Earth Planet. Sci. Lett.* 499:13–22

Cao M, Evans NJ, Reddy SM, Fougerouse D, Hollings P, et al. 2019. Micro- and nano-scale textural and compositional zonation in plagioclase at the Black Mountain porphyry Cu deposit: implications for magmatic processes. *Am. Mineral.* 104(3):391–402

Cashman KV, Sparks RSJ, Blundy JD. 2017. Vertically extensive and unstable magmatic systems: a unified view of igneous processes. *Science* 355(6331):eaag3055

Chakraborty S. 2010. Diffusion coefficients in olivine, wadsleyite and ringwoodite. *Rev. Mineral. Geochem.* 72:603–39

Chamberlain KJ, Morgan DJ, Wilson CJN. 2014. Timescales of mixing and mobilisation in the Bishop Tuff magma body: perspectives from diffusion chronometry. *Contrib. Mineral. Petrol.* 168(1):1034

Chambers M, Memeti V, Eddy MP, Schoene B. 2020. Half a million years of magmatic history recorded in a K-feldspar megacryst of the Tuolumne Intrusive Complex, California, USA. *Geology* 48(4):400–4

Cheng L, Costa F. 2019. Statistical analysis of crystal populations and links to volcano deformation for more robust estimates of magma replenishment volumes. *Geology* 47:1171–75

Cheng L, Costa F, Bergantz G. 2020. Linking fluid dynamics and olivine crystal scale zoning during simulated magma intrusion. *Contrib. Mineral. Petrol.* 175(6):53

Cheng L, Costa F, Carniel R. 2017. Unraveling the presence of multiple plagioclase populations and identification of representative two-dimensional sections using a statistical and numerical approach. *Am. Mineral.* 102(9):1894–905

Cherniak DJ. 1995. Diffusion of lead in plagioclase and K-feldspar: an investigation using Rutherford Backscattering and Resonant Nuclear Reaction Analysis. *Contrib. Mineral. Petrol.* 120(3–4):358–71

Cherniak DJ. 1996. Strontium diffusion in sanidine and albite, and general comments on strontium diffusion in alkali feldspars. *Geochim. Cosmochim. Acta* 60(24):5037–43

Cherniak DJ. 1998. Pb diffusion in clinopyroxene. *Chem. Geol.* 150(1–2):105–17

Cherniak DJ. 2001. Pb diffusion in Cr diopside, augite, and enstatite, and consideration of the dependence of cation diffusion in pyroxene on oxygen fugacity. *Chem. Geol.* 177(3–4):381–97

Cherniak DJ. 2002. Ba diffusion in feldspar. *Geochim. Cosmochim. Acta* 66(9):1641–50

Cherniak DJ. 2003. REE diffusion in feldspar. *Chem. Geol.* 193(1–2):25–41

Cherniak DJ. 2010. REE diffusion in olivine. *Am. Mineral.* 95(2–3):362–68

Cherniak DJ, Hanchar JM, Watson EB. 1997. Rare-earth diffusion in zircon. *Chem. Geol.* 134(4):289–301

Cherniak DJ, Liang Y. 2007. Rare earth element diffusion in natural enstatite. *Geochim. Cosmochim. Acta* 71(5):1324–40

Cherniak DJ, Liang Y. 2012. Ti diffusion in natural pyroxene. *Geochim. Cosmochim. Acta* 98:31–47

Cherniak DJ, Liang Y. 2014. Titanium diffusion in olivine. *Geochim. Cosmochim. Acta* 147:43–57

Cherniak DJ, Van Orman JA. 2014. Tungsten diffusion in olivine. *Geochim. Cosmochim. Acta* 129:1–12

Cherniak DJ, Watson EB. 1994. A study of strontium diffusion in plagioclase using Rutherford backscattering spectroscopy. *Geochim. Cosmochim. Acta* 58(23):5179–90

Cherniak DJ, Watson EB. 2001. Pb diffusion in zircon. *Chem. Geol.* 172(1–2):5–24

Cherniak DJ, Watson EB, Wark DA. 2007. Ti diffusion in quartz. *Chem. Geol.* 236(1–2):65–74

Coleman DS, Gray W, Glazner AF. 2004. Rethinking the emplacement and evolution of zoned plutons: geochronologic evidence for incremental assembly of the Tuolumne Intrusive Suite, California. *Geology* 32(5):433–36

Condomines M, Gauthier PJ, Sigmarsson O. 2003. Timescales of magma chamber processes and dating of young volcanic rocks. *Rev. Mineral. Geochem.* 52:125–74

Coogan LA, Hain A, Stahl S, Chakraborty S. 2005a. Experimental determination of the diffusion coefficient for calcium in olivine between 900°C and 1500°C. *Geochim. Cosmochim. Acta* 69(14):3683–94

Coogan LA, Kasemann SA, Chakraborty S. 2005b. Rates of hydrothermal cooling of new oceanic upper crust derived from lithium-geospeedometry. *Earth Planet. Sci. Lett.* 240:415–24

Cooper KM. 2015. Timescales of crustal magma reservoir processes: insights from U-series crystal ages. *Geol. Soc. Lond. Spec. Publ.* 422(1):141–74

Cooper KM. 2019. Time scales and temperatures of crystal storage in magma reservoirs: implications for magma reservoir dynamics. *Philos. Trans. R. Soc. A* 377(2139):20180009

Cooper KM, Kent AJR. 2014. Rapid remobilization of magmatic crystals kept in cold storage. *Nature* 506(7489):480–83

Cooper KM, Reid MR. 2008. Uranium-series crystal ages. *Rev. Mineral. Geochem.* 69(1):479–544

Cooper KM, Till CB, Kent AJR, Costa F, Rubin AE, et al. 2017. Response to Comment on "Rapid cooling and cold storage in a silicic magma reservoir recorded in individual crystals." *Science* 358:2016–18

Costa F. 2008. Chapter 1 residence times of silicic magmas associated with calderas. *Dev. Volcanol.* 10:1–55

Costa F, Dohmen R, Chakraborty S. 2008. Time scales of magmatic processes from modeling the zoning patterns of crystals. *Rev. Mineral. Geochem.* 69(1):545–94

Costa F, Dungan M. 2005. Short time scales of magmatic assimilation from diffusion modeling of multiple elements in olivine. *Geology* 33(10):837–40

Costa F, Morgan D. 2010. Time constraints from chemical equilibration in magmatic crystals. See Dosseto et al. 2010, pp. 125–59

Costa F, Shea T, Ubide T. 2020. Diffusion chronometry and the timescales of magmatic processes. *Nat. Rev. Earth Environ.* 1(4):201–14

Crank J. 1975. *The Mathematics of Diffusion*. Oxford, UK: Oxford Univ. Press

Davidson JP, Morgan DJ, Charlier BLA, Harlou R, Hora JM. 2007. Microsampling and isotopic analysis of igneous rocks: implications for the study of magmatic systems. *Annu. Rev. Earth Planet. Sci.* 35:273–311

de Maisonneuve CB, Costa F, Huber C, Vonlanthen P, Bachmann O, Dungan MA. 2016. How do olivines record magmatic events? Insights from major and trace element zoning. *Contrib. Mineral. Petrol.* 171(6):56

Demouchy S, Mackwell S. 2006. Mechanisms of hydrogen incorporation and diffusion in iron-bearing olivine. *Phys. Chem. Miner.* 33(5):347–55

Di Stefano F, Mollo S, Ubide T, Petrone CM, Caulfield J, et al. 2020. Mush cannibalism and disruption recorded by clinopyroxene phenocrysts at Stromboli volcano: new insights from recent 2003–2017 activity. *Lithos* 360–361:105440

Dodson MH. 1973. Closure temperature in cooling geochronological and petrological systems. *Contrib. Mineral. Petrol.* 40(3):259–74

Dohmen R, Chakraborty S. 2007. Fe–Mg diffusion in olivine II: point defect chemistry, change of diffusion mechanisms and a model for calculation of diffusion coefficients in natural olivine. *Phys. Chem. Miner.* 34(6):409–30

Dohmen R, Kasemann SA, Coogan L, Chakraborty S. 2010. Diffusion of Li in olivine. Part I: experimental observations and a multi species diffusion model. *Geochim. Cosmochim. Acta* 74(1):274–92

Dohmen R, Ter Heege JH, Becker HW, Chakraborty S. 2016. Fe-Mg interdiffusion in orthopyroxene. *Am. Mineral.* 101(10):2210–21

Dosseto A, Turner SP, Van Orman JA, eds. 2010. *Timescales of Magmatic Processes: From Core to Atmosphere*. Oxford, UK: Wiley-Blackwell

Druitt TH, Costa F, Deloule E, Dungan M, Scaillet B. 2012. Decadal to monthly timescales of magma transfer and reservoir growth at a caldera volcano. *Nature* 482(7383):77–80

Fabbro GN, Druitt TH, Costa F. 2017. Storage and eruption of silicic magma across the transition from dominantly effusive to caldera-forming states at an arc volcano (Santorini, Greece). *J. Petrol.* 58(12):2429–64

Flaherty T, Druitt TH, Tuffen H, Higgins MD, Costa F, Cadoux A. 2018. Multiple timescale constraints for high-flux magma chamber assembly prior to the Late Bronze Age eruption of Santorini (Greece). *Contrib. Mineral. Petrol.* 173(9):75

Foland KA. 1994. Argon diffusion in feldspars. In *Feldspars and Their Reactions*, ed. I Parsons, pp. 415–47. Dordrecht, Neth.: Kluwer

Ganguly J. 2002. Diffusion kinetics in minerals: principles and applications to tectono-metamorphic processes. *EMU Notes Mineral.* 4:271–309

Ganguly J, Ito M, Zhang X. 2007. Cr diffusion in orthopyroxene: experimental determination, ^{53}Mn–^{53}Cr thermochronology, and planetary applications. *Geochim. Cosmochim. Acta* 71(15):3915–25

Giletti BJ, Shanahan TM. 1997. Alkali diffusion in plagioclase feldspar. *Chem. Geol.* 139(1–4):3–20
Girona T, Costa F. 2013. DIPRA: a user-friendly program to model multi-element diffusion in olivine with applications to timescales of magmatic processes. *Geochem. Geophys. Geosyst.* 14(2):422–31
Gualda GAR, Pamukcu AS, Ghiorso MS, Anderson AT, Sutton SR, Rivers ML. 2012. Timescales of quartz crystallization and the longevity of the Bishop giant magma body. *PLOS ONE* 7(5):e37492
Halliday AN, Mahood GA, Holden P, Metz JM, Dempster TJ, Davidson JP. 1989. Evidence for long residence times of rhyolitic magma in the Long Valley magmatic system: the isotopic record in precaldera lavas of Glass Mountain. *Earth Planet. Sci. Lett.* 94(3–4):274–90
Handley HK, Reagan M, Gertisser R, Preece K, Berlo K, et al. 2018. Timescales of magma ascent and degassing and the role of crustal assimilation at Merapi volcano (2006–2010), Indonesia: constraints from uranium-series and radiogenic isotopic compositions. *Geochim. Cosmochim. Acta* 222:34–52
Ingrin J, Peipei Z. 2016. Hydrogen diffusion in Zircon. *Geophys. Res. Abstr.* 18:EGU2016-7148
Ito M, Ganguly J. 2006. Diffusion kinetics of Cr in olivine and ^{53}Mn–^{53}Cr thermochronology of early solar system objects. *Geochim. Cosmochim. Acta* 70(3):799–809
Johnson EA, Rossman GR. 2013. The diffusion behavior of hydrogen in plagioclase feldspar at 800–1000 C: implications for re-equilibration of hydroxyl in volcanic phenocrysts. *Am. Mineral.* 98(10):1779–87
Jollands MC, Bloch E, Müntener O. 2020. New Ti-in-quartz diffusivities reconcile natural Ti zoning with time scales and temperatures of upper crustal magma reservoirs. *Geology* 48(7):654–57
Kahl M, Chakraborty S, Costa F, Pompilio M. 2011. Dynamic plumbing system beneath volcanoes revealed by kinetic modeling, and the connection to monitoring data: an example from Mt. Etna. *Earth Planet. Sci. Lett.* 308(1–2):11–22
Kahl M, Chakraborty S, Costa F, Pompilio M, Liuzzo M, Viccaro M. 2013. Compositionally zoned crystals and real-time degassing data reveal changes in magma transfer dynamics during the 2006 summit eruptive episodes of Mt. Etna. *Bull. Volcanol.* 75(2):692
Karakas O, Wotzlaw J-F, Guillong M, Ulmer P, Brack P, et al. 2019. The pace of crustal-scale magma accretion and differentiation beneath silicic caldera volcanoes. *Geology* 47(8):719–23
Kent AJR, Cooper KM. 2018. How well do zircons record the thermal evolution of magmatic systems? *Geology* 46(2):111–14
Kohn MJ, Penniston-Dorland SC. 2017. Diffusion: obstacles and opportunities in petrochronology. *Rev. Mineral. Geochem.* 83(1):103–52
Kronenberg AK, Kirby SH, Aines RD, Rossman GR. 1986. Solubility and diffusional uptake of hydrogen in quartz at high water pressures: implications for hydrolytic weakening. *J. Geophys. Res.* 91(B12):12723–41
MacDougall D 2008. *Nature's Clocks. How Scientists Measure the Age of Almost Everything*. Berkeley, CA: University Calif. Press
Mahood GA, Halliday AN. 1990. Second reply to comment of R.S.J. Sparks, H.E. Huppert and C.J.N. Wilson on "Evidence for long residence times of rhyolitic magma in the Long Valley magmatic system: the isotopic record in the precaldera lavas of Glass Mountain." *Earth Planet. Sci. Lett.* 99(4):395–99
Manzini M, Bouvier AS, Baumgartner LP, Müntener O, Rose-Koga EF, et al. 2017. Weekly to monthly time scale of melt inclusion entrapment prior to eruption recorded by phosphorus distribution in olivine from mid-ocean ridges. *Geology* 45(12):1059–62
Miller CF. 2016. Eruptible magma. *PNAS* 113(49):13941–43
Miller JS, Matzel JEP, Miller CF, Burgess SD, Miller RB. 2007. Zircon growth and recycling during the assembly of large, composite arc plutons. *J. Volcanol. Geotherm. Res.* 167(1–4):282–99
Müller T, Dohmen R, Becker HW, ter Heege JH, Chakraborty S. 2013. Fe–Mg interdiffusion rates in clinopyroxene: experimental data and implications for Fe–Mg exchange geothermometers. *Contrib. Mineral. Petrol.* 166(6):1563–76
Mutch EJF, Maclennan J, Holland TJB, Buisman I. 2019. Millennial storage of near-Moho magma. *Science* 365(6450):260–64
Oeser M, Dohmen R, Horn I, Schuth S, Weyer S. 2015. Processes and time scales of magmatic evolution as revealed by Fe–Mg chemical and isotopic zoning in natural olivines. *Geochim. Cosmochim. Acta* 154:130–50
Pankhurst MJ, Morgan DJ, Thordarson T, Loughlin SC. 2018. Magmatic crystal records in time, space, and process, causatively linked with volcanic unrest. *Earth Planet. Sci. Lett.* 493:231–41

Petry C, Chakraborty S, Palme H. 2004. Experimental determination of Ni diffusion coefficients in olivine and their dependence on temperature, composition, oxygen fugacity, and crystallographic orientation. *Geochim. Cosmochim. Acta* 68(20):4179–88

Putirka KD. 2008. Thermometers and barometers for volcanic systems. *Rev. Mineral. Geochem.* 69:61–120

Rasmussen DJ, Plank TA, Roman DC, Power JA, Bodnar RJ, Hauri EH. 2018. When does eruption run-up begin? Multidisciplinary insight from the 1999 eruption of Shishaldin volcano. *Earth Planet. Sci. Lett.* 486:1–14

Reid MR. 2003. Timescales of magma transfer and storage in the crust. In *The Crust*, Vol. 3, ed. RL Rudnick, pp. 167–93. New York: Elsevier

Reid MR, Coath CD. 2000. In situ U-Pb ages of zircons from the Bishop Tuff: no evidence for long crystal residence times. *Geology* 28(5):443–46

Reid MR, Coath CD, Harrison TM, McKeegan KD. 1997. Prolonged residence times for the youngest rhyolites associated with Long Valley Caldera: ^{230}Th–^{238}U ion microprobe dating of young zircons. *Earth Planet. Sci. Lett.* 150(1–2):27–39

Reiners PW. 2009. Nonmonotonic thermal histories and contrasting kinetics of multiple thermochronometers. *Geochim. Cosmochim. Acta* 73(12):3612–29

Reiners PW, Carlson RW, Renne PR, Cooper KM, Granger DE, et al. 2018. *Geochronology and Thermochronology*. Hoboken, NJ: Wiley

Richet P. 1999. *A Natural History of Time*. Chicago: Chicago Univ. Press

Rubin AE, Cooper KM, Till CB, Kent AJR, Costa F, et al. 2017. Rapid cooling and cold storage in a silicic magma reservoir recorded in individual crystals. *Science* 356(6343):1154–56

Ruprecht P, Plank T. 2013. Feeding andesitic eruptions with a high-speed connection from the mantle. *Nature* 500(7460):68–72

Ruth DCS, Costa F, Bouvet de Maisonneuve C, Franco L, Cortés JA, Calder ES. 2018. Crystal and melt inclusion timescales reveal the evolution of magma migration before eruption. *Nat. Commun.* 9(1):2657

Schaltegger U, Davies JHFL. 2017. Petrochronology of zircon and baddeleyite in igneous rocks: reconstructing magmatic processes at high temporal resolution. *Rev. Mineral. Geochem.* 83(1):297–328

Schmitt AK. 2011. Uranium series accessory crystal dating of magmatic processes. *Annu. Rev. Earth Planet. Sci.* 39:321–49

Schmitt AK, Vazquez JA. 2017. Secondary ionization mass spectrometry analysis in petrochronology. *Rev. Mineral. Geochem.* 83(1):199–230

Schoene B, Schaltegger U, Brack P, Latkoczy C, Stracke A, Günther D. 2012. Rates of magma differentiation and emplacement in a ballooning pluton recorded by U–Pb TIMS-TEA, Adamello batholith, Italy. *Earth Planet. Sci. Lett.* 355–356:162–73

Shea T, Costa F, Krimer D, Hammer JE. 2015a. Accuracy of timescales retrieved from diffusion modeling in olivine: a 3D perspective. *Am. Mineral.* 100(10):2026–42

Shea T, Lynn KJ, Garcia MO. 2015b. Cracking the olivine zoning code: distinguishing between crystal growth and diffusion. *Geology* 43(10):935–38

Sigmarsson O. 1996. Short magma chamber residence time at an Icelandic volcano inferred from U-series disequilibria. *Nature* 382:440–42

Sigmundsson F, Hreinsdóttir S, Hooper A, Árnadóttir T, Pedersen R, et al. 2010. Intrusion triggering of the 2010 Eyjafjallajökull explosive eruption. *Nature* 468(7322):426–32

Simon J, Reid M. 2005. The pace of rhyolite differentiation and storage in an 'archetypical' silicic magma system, Long Valley, California. *Earth Planet. Sci. Lett.* 235(1–2):123–40

Sims KWW, Pichat S, Reagan MK, Kyle PR, Dulaiova H, et al. 2013. On the time scales of magma genesis, melt evolution, crystal growth rates and magma degassing in the Erebus volcano magmatic system using the ^{238}U, ^{235}U and ^{232}Th decay series. *J. Petrol.* 54(2):235–71

Sliwinski JT, Kueter N, Marxer F, Ulmer P, Guillong M, Bachmann O. 2018. Controls on lithium concentration and diffusion in zircon. *Chem. Geol.* 501:1–11

Stalder R, Skogby H. 2003. Hydrogen diffusion in natural and synthetic orthopyroxene. *Phys. Chem. Miner.* 30(1):12–19

Sundvall R, Skogby H, Stalder R. 2009. Dehydration-hydration mechanisms in synthetic Fe-poor diopside. *Eur. J. Mineral.* 21(1):17–26

Tailby ND, Cherniak DJ, Watson EB. 2018. Al diffusion in quartz. *Am. Mineral.* 103(6):839–47
Tang M, Rudnick RL, McDonough WF, Bose M, Goreva Y. 2017. Multi-mode Li diffusion in natural zircons: evidence for diffusion in the presence of step-function concentration boundaries. *Earth Planet. Sci. Lett.* 474:110–19
Till CB, Vazquez JA, Boyce JW. 2015. Months between rejuvenation and volcanic eruption at Yellowstone caldera, Wyoming. *Geology* 43(8):695–98
Trail D, Cherniak DJ, Watson EB, Harrison TM, Weiss BP, Szumila I. 2016. Li zoning in zircon as a potential geospeedometer and peak temperature indicator. *Contrib. Mineral. Petrol.* 171(3):25
Turner S, Costa F. 2007. Measuring timescales of magmatic evolution. *Elements* 3(4):267–72
Ubide T, Caulfield J, Brandt C, Bussweiler Y, Mollo S, et al. 2019. Deep magma storage revealed by multi-method elemental mapping of clinopyroxene megacrysts at Stromboli Volcano. *Front. Earth Sci.* 7:239
Van Orman JA, Cherniak DJ, Kita NT. 2014. Magnesium diffusion in plagioclase: dependence on composition, and implications for thermal resetting of the ^{26}Al–^{26}Mg early solar system chronometer. *Earth Planet. Sci. Lett.* 385:79–88
Van Orman JA, Grove TL, Shimizu N. 2001. Rare earth element diffusion in diopside: influence of temperature, pressure, and ionic radius, and an elastic model for diffusion in silicates. *Contrib. Mineral. Petrol.* 141(6):687–703
Verhoogen J. 1952. Ionic diffusion and electrical conductivity in quartz. *Am. Mineral.* 37(7–8):637–55
Wark DA, Hildreth W, Spear FS, Cherniak DJ, Watson EB. 2007. Pre-eruption recharge of the Bishop magma system. *Geology* 35(3):235–38
Wartho JA, Kelley SP, Elphick SC. 2013. Ar diffusion and solubility measurements in plagioclases using the ultra-violet laser depth-profiling technique. *Geol. Soc. Spec. Publ.* 378(1):137–54
Watson EB, Cherniak DJ, Holycross ME. 2015. Diffusion of phosphorus in olivine and molten basalt. *Am. Mineral.* 100(10):2053–65
Wilson CJN, Charlier BLA. 2009. Rapid rates of magma generation at contemporaneous magma systems, Taupo volcano, New Zealand: insights from U–Th model-age spectra in zircons. *J. Petrol.* 50(5):875–907
Wilson CJN, Morgan DJ, Charlier BLA, Barker SJ. 2017. Comment on "Rapid cooling and cold storage in a silicic magma reservoir recorded in individual crystals." *Science* 358(6370):eaap8429
Zhang Y. 2008. *Geochemical Kinetics*. Princeton, NJ: Princeton Univ. Press
Zhang Y, Cherniak DJ. 2010. Diffusion in minerals and melts: introduction. *Rev. Mineral. Geochem.* 72(1):1–4

Annual Review
of Earth and
Planetary Sciences
Volume 49, 2021

Contents

Errata

An online log of corrections to *Annual Review of Earth and Planetary Sciences* articles may be found at http://www.annualreviews.org/errata/earth